Electrical control of phonon-mediated spin relaxation rate in semiconductor quantum dots: Rashba versus Dresselhaus spin-orbit coupling

Sanjay Prabhakar,[1] Roderick Melnik,[1,2] and Luis L. Bonilla[2]
[1]*M [2]NeT Laboratory, Wilfrid Laurier University, Waterloo N2L 3C5, Ontario, Canada*
[2]*Gregorio Millan Institute, Universidad Carlos III de Madrid, 28911 Leganes, Spain*
(Received 29 March 2013; revised manuscript received 15 May 2013; published 7 June 2013)

In symmetric quantum dots (QDs), it is well known that the spin hot spot (i.e., the cusplike structure due to the presence of degeneracy near the level or anticrossing point) is present for the pure Rashba case but is absent for the pure Dresselhaus case [Bulaev and Loss, Phys. Rev. Lett. **95**, 076805 (2005)]. Since the Dresselhaus spin-orbit coupling dominates over the Rashba spin-orbit coupling in GaAs and GaSb QDs, it is important to find the exact location of the spin hot spot or the cusplike structure even for the pure Dresselhaus case. In this paper, we present analytical and numerical results that show that the spin hot spot can also be seen for the pure Dresselhaus spin-orbit coupling case by inducing large anisotropy through external gates. At or nearby the spin hot spot, the spin transition rate increases and the decoherence time decreases by several orders of magnitude compared to the case with no spin hot spot. Thus one should avoid such locations when designing QD spin based transistors for possible implementation in quantum logic gates, solid-state quantum computing, and quantum information processing. It is also possible to extract the exact experimental data [Amasha, MacLean, Radu, Zumbühl, Kastner, Hanson, and Gossard, Phys. Rev. Lett. **100**, 046803 (2008] for the phonon mediated spin-flip rates from our developed theoretical model.

DOI: 10.1103/PhysRevB.87.235202 PACS number(s): 73.21.La, 71.70.Ej, 72.25.Rb

I. INTRODUCTION

Manipulation of a single electron spin with the application of gate controlled electric fields in confined semiconductor quantum dots (QDs) is a promising way for developing spin based quantum logic gates, spin memory devices for various quantum information processing applications.[1–12] Sufficiently short gate operation time combined with long decoherence time is one of the requirements for quantum computing.[1,13,14] When a qubit is operated on by a classical bit, then its decay time is given by a spin-relaxation time which is also supposed to be longer than the minimum time required to execute one quantum gate operation.[2,13,15–17] Long spin relaxations have been measured experimentally in both symmetric and asymmetric QDs.[4,5,15] Balocchi *et al.*[18] have recently measured larger spin-relaxation times (30 ns) in GaAs QDs. More specifically, both isotropic and anisotropic spin relaxations can be tuned with spin-orbit coupling by choosing the growth direction parallel to the crystallographic axis [001], [110], and [111] of III-V zinc-blende semiconductor QDs.[6,18–20] In addition to the lengthening spin coherence time, the electric-field tuning of spin relaxation forms the basis for turning the spin current on and off in some spin transistor proposals that can help to initialize electron-spin based quantum computers.[16,21] These experimental studies confirm that the manipulation of spin-flip rates mediated by phonons due to spin-orbit coupling is an important ingredient for the design of robust spintronics logic devices. The spin-orbit coupling is mainly dominated by the Rashba[22] and the linear Dresselhaus[23] terms in III-V semiconductor QDs.[17,24–33] The Rashba spin-orbit coupling arises from structural inversion asymmetry along the growth direction, while the Dresselhaus spin-orbit coupling arises from the bulk inversion asymmetry of the crystal lattice.[22,23]

In Refs. 34 and 35, the authors report that the cusplike structure in the phonon mediated spin transition rate can be seen for the pure Rashba case. For the pure Dresselhaus case, the spin transition rate is a monotonous function of the magnetic fields and QD radii. Since the Dresselhaus spin-orbit coupling dominates over the Rashba spin-orbit coupling in some materials such as GaAs and GaSb QDs,[25] it is important to find the exact location of the spin hot spot or the cusplike structure even for the pure Dresselhaus case. The cusplike structure implies shorter spin-relaxation and decoherence time, which is hazardous for spin based applications such as quantum logic gates, solid-state quantum computing, and quantum information processing. For these applications, the spin hot spot in the phonon mediated spin-relaxation rate is something to avoid during the design of QD spin based transistors. Very recently, the authors in Ref. 36 measured the spin hot spot in the phonon mediated spin-relaxation rate in silicon QDs with the application of tuning very weak spin-orbit coupling when Zeeman energy and valley splittings induce degeneracy. At the spin hot spot in silicon QDs, the dramatic rate enhancement decreases the decoherence time, which is not supposed to be the ideal location for the qubit operation.[37–40] In this paper, we obtain analytical and numerical results for the behavior of the spin-relaxation rate in anisotropic III-V semiconductor QDs. We show that the spin hot spot in the phonon mediated spin transition rate can be seen for the pure Dresselhaus case by creating large anisotropy through external gates. Note that such a location (the spin hot spot) is hazardous for quantum computing and quantum information processing and must therefore be avoided during the design of spin based transistors.

The paper is organized as follows. In Sec. II, we develop a theoretical model for anisotropic spin relaxation mediated by piezo phonons that will allow us to investigate the interplay between the Rashba and the linear Dresselhaus spin-orbit coupling in QDs. In Sec. III, we provide details of the diagonalization technique used for finding the energy spectrum and the matrix elements of the phonon mediated spin transition rate in QDs. In Sec. IV, we plot both isotropic and anisotropic spin-relaxation rates vs magnetic fields and QD radii for the

pure Rashba and the pure Dresselhaus case in III-V semiconductor materials of zinc-blende structures such as GaAs, GaSb, InAs, and InSb. Finally, in Sec. V, we summarize our results.

II. THEORETICAL MODEL

We consider two-dimensional anisotropic semiconductor QDs in the presence of a magnetic field along the growth direction. The total Hamiltonian of an electron in anisotropic QDs including spin-orbit interactions can be written as[26,34,42] $H = H_{xy} + H_{\rm SO}$, where $H_{\rm SO} = H_R + H_D$ is the Hamiltonian associated with the Rashba-Dresselhaus spin-orbit coupling and H_{xy} is the Hamiltonian of the electron in anisotropic QDs. H_{xy} can be written as

$$H_{xy} = \frac{\vec{P}^2}{2m} + \frac{1}{2}m\omega_o^2(ax^2 + by^2) + \frac{1}{2}g_o\mu_B\sigma_z B, \qquad (1)$$

where $\vec{P} = \vec{p} + e\vec{A}$ is the kinetic momentum operator, $\vec{p} = -i\hbar(\partial_x,\partial_y,0)$ is the canonical momentum operator, $\vec{A} = B(-y\sqrt{b},x\sqrt{a},0)/(\sqrt{a}+\sqrt{b})$ is the vector potential in the asymmetric gauge, m is the effective mass, μ_B is the Bohr magneton, $\vec{\sigma} = (\sigma_x,\sigma_y,\sigma_z)$ are the Pauli spin matrices, g_0 is the bulk g factor, $\omega_0 = \hbar/(m\ell_0^2)$ is the parabolic confining potential, and ℓ_0 is the radius of the QDs. The energy spectrum of H_{xy} can be written as[26,43]

$$\varepsilon^0_{n_+,n_-,\pm} = (n_+ + n_- + 1)\hbar\omega_+ + (n_+ - n_-)\hbar\omega_- \pm \frac{\Delta}{2}, \qquad (2)$$

where $\omega_\pm = \frac{1}{2}[\omega_c^2 + \omega_0^2(\sqrt{a}\pm\sqrt{b})^2]^{1/2}$, $\Delta = g_0\mu_B B$, and $n_\pm$ are the eigenvalues of the Fock-Darwin number operators $a_\pm^\dagger a_\pm$. Here, $a_\pm$ and $a_\pm^\dagger$ are the usual annihilation and creation operators. Also, we label the Fock-Darwin states as $|n_+,n_-,\pm\rangle$, with $\pm$ being the eigenvalues of the Pauli spin matrix along the z direction.[24,26]

Finally, $H_{\rm SO}$ can be written as[26]

$$H_{\rm SO} = \frac{\alpha_R}{\hbar}(\sigma_x P_y - \sigma_y P_x) + \frac{\alpha_D}{\hbar}(-\sigma_x P_x + \sigma_y P_y), \qquad (3)$$

where

$$\alpha_R = \gamma_R eE, \quad \alpha_D = 0.78\gamma_D\left(\frac{2meE}{\hbar^2}\right)^{2/3}. \qquad (4)$$

Here γ_R and γ_D are the Rashba and Dresselhaus spin-orbit coefficients. In Fig. 1, we have plotted the contribution of the Rashba-Dresselhaus spin-orbit coupling (α_R/α_D) with the variation of applied electric fields (E) along the z direction. It can be seen that the Rashba spin-orbit coupling dominates in InAs and InSb QDs, whereas the Dresselhaus spin-orbit coupling dominates in GaAs and GaSb QDs. In Sec. IV we will focus our investigation on the phonon mediated spin relaxation in both symmetric and asymmetric QDs.

The Hamiltonian Eq. (3) can be written in terms of raising and lowering operators as

$$\begin{aligned} H_{\rm SO} = {} & \alpha_R(1+i)[b^{1/4}\kappa_+(s_+ - i)a_+ + b^{1/4}\kappa_+(s_- + i)a_- \\ & + a^{1/4}\eta_-(i - s_-)a_+ + a^{1/4}\eta_-(i + s_+)a_-] \\ & + \alpha_D(1+i)[a^{1/4}\kappa_-(i - s_-)a_+ + a^{1/4}\kappa_-(i + s_+)a_- \\ & + b^{1/4}\eta_+(-i + s_+)a_+ + b^{1/4}\eta_+(i + s_-)a_-] + \text{H.c.}, \end{aligned} \qquad (5)$$

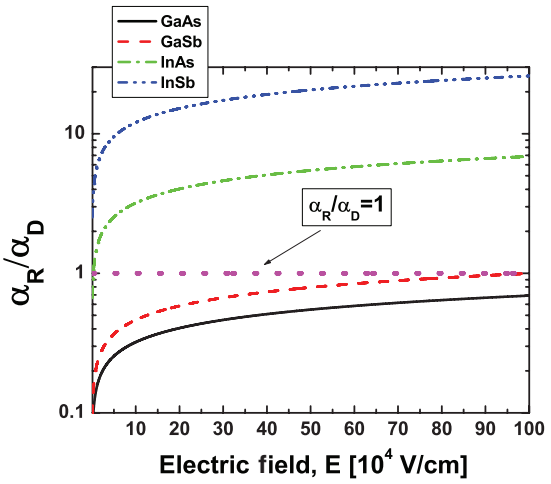

FIG. 1. (Color online) Interplay between Rashba-Dresselhaus spin-orbit coupling vs the applied electric field along the z direction. The Rashba spin-orbit coupling is seen to dominate in InAs and InSb QDs, whereas the Dresselhaus spin-orbit coupling is seen to dominate in GaAs and GaSb QDs.

where

$$s_\pm = \frac{\omega_+}{\omega_c\left(\frac{b}{a}\right)^{\frac{1}{4}}}\left\{\sqrt{\frac{b}{a}} - 1 \pm \left[\frac{\omega_c^2\sqrt{\frac{b}{a}}}{\omega_+^2} + \left(1 - \sqrt{\frac{b}{a}}\right)^2\right]^{\frac{1}{2}}\right\}, \qquad (6)$$

$$\kappa_\pm = \frac{1}{2(s_+ - s_-)}\left\{\frac{1}{\ell}\sigma_x \pm i\frac{eB\ell}{\hbar}\left(\frac{1}{\sqrt{a}+\sqrt{b}}\right)\sigma_y\right\}, \qquad (7)$$

$$\eta_\pm = \frac{1}{2(s_+ - s_-)}\left\{\frac{1}{\ell}\sigma_y \pm i\frac{eB\ell}{\hbar}\left(\frac{1}{\sqrt{a}+\sqrt{b}}\right)\sigma_x\right\}. \qquad (8)$$

H.c. represents the Hermitian conjugate, $\ell = \sqrt{\hbar/m\Omega}$ is the hybrid orbital length, and $\Omega = \sqrt{\omega_0^2 + \omega_c^2/(\sqrt{a}+\sqrt{b})^2}$.

At low electric fields and small QD radii, we treat the Hamiltonian associated with the Rashba and linear Dresselhaus spin-orbit coupling as a perturbation. Using second-order nondegenerate perturbation theory, the energy spectrum of the two lowest electron-spin states in QDs (for details, see Ref. 43) is given by

$$\varepsilon_{0,0,+} = \hbar\varpi_+ - \frac{\alpha_R^2\xi_+ + \alpha_D^2\varsigma_+}{\hbar\omega_x - \Delta} - \frac{\alpha_R^2\varsigma_- + \alpha_D^2\xi_-}{\hbar\omega_y - \Delta}, \qquad (9)$$

$$\varepsilon_{0,0,-} = \hbar\varpi_- - \frac{\alpha_R^2\varsigma_+ + \alpha_D^2\xi_+}{\hbar\omega_x + \Delta} - \frac{\alpha_R^2\xi_- + \alpha_D^2\varsigma_-}{\hbar\omega_y + \Delta}, \qquad (10)$$

where $\varpi_\pm = \omega_+ \pm \omega_z/2$, $\omega_z = \Delta/\hbar$ is the Zeeman frequency, $\omega_x = \omega_+ + \omega_-$, and $\omega_y = \omega_+ - \omega_-$. Also,

$$\xi_\pm = \frac{1}{2(s_+ - s_-)}\left\{\pm\frac{1}{s_\pm}\alpha_\pm^2 + 2\alpha_\pm\beta_\pm \mp \frac{1}{s_\mp}\beta_\pm^2\right\}, \qquad (11)$$

$$\varsigma_\pm = \frac{1}{2(s_+ - s_-)}\left\{\pm\frac{1}{s_\pm}\alpha_\mp^2 - 2\alpha_\mp\beta_\mp \mp \frac{1}{s_\mp}\beta_\mp^2\right\}, \qquad (12)$$

$$\alpha_\pm = a^{1/4}\left\{\frac{1}{\ell} \pm \frac{eB\ell}{\hbar}\frac{1}{(\sqrt{a}+\sqrt{b})}\right\}, \qquad (13)$$

$$\beta_\pm = b^{1/4}\left\{\frac{1}{\ell} \pm \frac{eB\ell}{\hbar}\frac{1}{(\sqrt{a}+\sqrt{b})}\right\}. \qquad (14)$$

We now turn to the calculation of the phonon induced spin-relaxation rate at absolute zero temperature between the two lowest energy states in QDs. Following Refs. 26,27,42, and 44, the interaction between the electron and piezo phonon can be written[45]

$$u_{ph}^{\mathbf{q}\alpha}(\mathbf{r},t)=\sqrt{\frac{\hbar}{2\rho V\omega_{\mathbf{q}\alpha}}}e^{i(\mathbf{q}\cdot\mathbf{r}-\omega_{q\alpha}t)}eA_{\mathbf{q}\alpha}b_{\mathbf{q}\alpha}^{\dagger}+\text{H.c.}, \quad (15)$$

where ρ is the crystal mass density and V is the volume of the QD. $b_{\mathbf{q}\alpha}^{\dagger}$ creates an acoustic phonon with wave vector $\mathbf{q}$ and polarization $\hat{e}_\alpha$, where $\alpha=l,t_1,t_2$ are chosen as one longitudinal and two transverse modes of the induced phonon in the dots. $A_{\mathbf{q}\alpha}=\hat{q}_i\hat{q}_k e\beta_{ijk}e_{\mathbf{q}\alpha}^{j}$ is the amplitude of the electric field created by phonon strain, where $\hat{\mathbf{q}}=\mathbf{q}/q$ and $e\beta_{ijk}=eh_{14}$ for $i\neq k, i\neq j, j\neq k$. The polarization directions of the induced phonon are $\hat{e}_l=(\sin\theta\cos\phi,\sin\theta\sin\phi,\cos\theta)$, $\hat{e}_{t_1}=(\cos\theta\cos\phi,\cos\theta\sin\phi,-\sin\theta)$, and $\hat{e}_{t_2}=(-\sin\phi,\cos\phi,0)$. Based on the Fermi golden rule, the phonon induced spin transition rate in the QDs is given by[26,44]

$$\frac{1}{T_1}=\frac{2\pi}{\hbar}\int\frac{d^3\mathbf{q}}{(2\pi)^3}\sum_{\alpha=l,t}|M(\mathbf{q}\alpha)|^2\delta(\hbar s_\alpha\mathbf{q}-\varepsilon_f+\varepsilon_i), \quad (16)$$

where s_l,s_t are the longitudinal and transverse acoustic phonon velocities in QDs. The matrix element $M(\mathbf{q}\alpha)=\langle\psi_i|u_{ph}^{\mathbf{q}\alpha}(\mathbf{r},t)|\psi_f\rangle$ with the emission of one phonon $\mathbf{q}\alpha$ has been calculated perturbatively and numerically.[41,44,46] Here $|\psi_i\rangle$ and $|\psi_f\rangle$ correspond to the initial and final states of the Hamiltonian H. Based on second-order nondegenerate perturbation theory, after long algebraic transformations, we have

$$\frac{1}{T_1}=c(|M_x|^2+|M_y|^2), \quad (17)$$

where

$$c=\frac{2(eh_{14})^2(g\mu_B B)^3}{35\pi\hbar^4\rho}\left(\frac{1}{s_l^5}+\frac{4}{3}\frac{1}{s_t^5}\right), \quad (18)$$

$$M_x=\frac{(is_-+1)\Xi_1(\hbar\omega_x+\Delta)+(-is_-+1)\Xi_3(\hbar\omega_x-\Delta)}{a^{1/4}[(\hbar\omega_x)^2-\Delta^2]}+\frac{(-is_++1)\Xi_2(\hbar\omega_y+\Delta)+(is_++1)\Xi_4(\hbar\omega_y-\Delta)}{a^{1/4}[(\hbar\omega_y)^2-\Delta^2]}, \quad (19)$$

$$M_y=\frac{(is_++1)\Xi_1(\hbar\omega_x+\Delta)+(-is_++1)\Xi_3(\hbar\omega_x-\Delta)}{b^{1/4}[(\hbar\omega_x)^2-\Delta^2]}+\frac{(is_--1)\Xi_2(\hbar\omega_y+\Delta)+(-is_--1)\Xi_4(\hbar\omega_y-\Delta)}{b^{1/4}[(\hbar\omega_y)^2-\Delta^2]}, \quad (20)$$

$$\Xi_1=\frac{\ell}{2(s_+-s_-)^2}\{\alpha_R[(s_++i)\beta_++(1-is_-)\alpha_+]+\alpha_D[(-s_--i)\alpha_-+(-1+is_+)\beta_-]\}, \quad (21)$$

$$\Xi_2=\frac{\ell}{2(s_+-s_-)^2}\{\alpha_R[(s_--i)\beta_++(1+is_+)\alpha_+]+\alpha_D[(s_+-i)\alpha_-+(1+is_-)\beta_-]\}, \quad (22)$$

$$\Xi_3=\frac{\ell}{2(s_+-s_-)^2}\{\alpha_R[(s_+-i)\beta_-+(-1-is_-)\alpha_-]+\alpha_D[(-s_-+i)\alpha_++(1+is_+)\beta_+]\}, \quad (23)$$

$$\Xi_4=\frac{\ell}{2(s_+-s_-)^2}\{\alpha_R[(s_-+i)\beta_-+(-1+is_+)\alpha_-]+\alpha_D[(s_++i)\alpha_++(-1+is_-)\beta_+]\}. \quad (24)$$

In the above expression, we use $c=c_lI_{xl}+2c_tI_{xt}$, where $c_\alpha=\frac{q^2e^2}{(2\pi)^2\hbar^2 s_\alpha}|\varepsilon_{q\alpha}|^2$, $|\varepsilon_{q\alpha}|^2=\frac{q^2\hbar}{2\rho\omega_{q\alpha}}$, and $q=\frac{g\mu_B B}{\hbar s_\alpha}$. Also, $g=\frac{\varepsilon_{0,0,-}-\varepsilon_{0,0,+}}{\mu_B B}$ is the Landé g factor. For longitudinal phonon modes,[13,44] we have $|A_{q,l}|^2=36h_{14}^2\cos^2\theta\sin^4\theta\sin^2\phi\cos^2\phi$, and thus we find $I_{xl}=16\pi h_{14}^2/35$. For transverse phonon modes, we have $|A_{q,t}|^2=2h_{14}^2[\cos^2\theta\sin^2\theta+\sin^4\theta(1-9\cos^2\theta)\sin^2\phi\cos^2\phi]$, and thus we find $I_{xt}=32\pi h_{14}^2/105$.

For isotropic QDs ($a=b=1$, $s_+=1$ and $s_-=-1$), the spin-relaxation rate is given by

$$\frac{1}{T_1}=\frac{2(eh_{14})^2(g\mu_B B)^3}{35\pi\hbar^4\rho}\left(\frac{1}{s_l^5}+\frac{4}{3}\frac{1}{s_t^5}\right)(|M_R|^2+|M_D|^2), \quad (25)$$

where M_R and M_D are the coefficients of matrix elements associated with the Rashba and Dresselhaus spin-orbit coupling in QDs and are given by

$$M_R=\frac{\alpha_R}{\sqrt{2}\hbar\Omega}\left[\frac{1}{1-\frac{\Delta}{\hbar(\Omega+\frac{\omega_c}{2})}}-\frac{1}{1+\frac{\Delta}{\hbar(\Omega-\frac{\omega_c}{2})}}\right], \quad (26)$$

$$M_D=\frac{\alpha_D}{\sqrt{2}\hbar\Omega}\left[\frac{1}{1+\frac{\Delta}{\hbar(\Omega+\frac{\omega_c}{2})}}-\frac{1}{1-\frac{\Delta}{\hbar(\Omega-\frac{\omega_c}{2})}}\right]. \quad (27)$$

Since $\Delta=g_0\mu_B B$ is negative, we see that the degeneracy only appears in the Rashba case [see the second term of Eq. (26)] and the degeneracy is absent in the Dresselhaus case. The degeneracy in the Rashba case induces the level crossing point and cusplike structure in the spin-flip rate in QDs. The spin-relaxation rate for isotropic QDs can be written in a more

convenient form as

$$\frac{1}{T_1} = \frac{2\,(eh_{14})^2\,(g\mu_B B)^3}{35\pi\hbar^4\rho}\left(\frac{1}{s_l^5}+\frac{4}{3}\frac{1}{s_t^5}\right)\frac{2\Delta^2 m^4}{\hbar^8} \times \left(\alpha_R^2+\alpha_D^2\right)\ell_0^8[1+O(\omega_c/\omega_o)^2]. \quad (28)$$

From Eq. (28), it is clear that the spin-flip rate vanishes like B^5 and ℓ_0^8 (see Ref. 26).

III. COMPUTATIONAL METHOD

We suppose that a QD is formed at the center of a 400×400-nm^2 geometry. Then we diagonalize the total Hamiltonian H numerically using the finite element method.[41] The geometry contains 24 910 elements. Since the geometry is much larger compared to the actual lateral size of the QD, we impose Dirichlet boundary conditions and find the eigenvalues, eigenfunctions, and the matrix elements $M(\mathbf{q}\alpha)$ of the total Hamiltonian H. From Figs. 2–7, the analytically obtained spin-flip rates from Eq. (17) (solid and dashed-dotted lines) are seen to be in excellent agreement with the numerical values (open circles and squares). The material constants are taken from Table I.

IV. RESULTS AND DISCUSSIONS

In Fig. 2, we compare theoretically obtained spin-flip rates from Eq. (17) to the experimentally reported values in Ref. 15. Theoretical and experimental data are in excellent agreement. Inset plots (from left to right) show realistic in-plane wave functions of QDs for the spin states $|0,0,+1/2\rangle$, $|0,0,-1/2\rangle$, and $|0,1,+1/2\rangle$. It can be seen that anisotropy breaks the in-plane rotational symmetry. As a result, we find that the in-plane wave functions of anisotropic QDs for the states $|0,1,+1/2\rangle$ split into two, which has a direct consequence on inducing

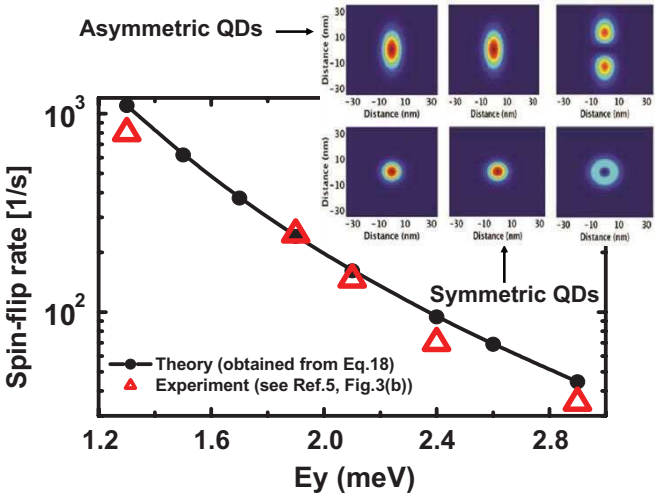

FIG. 2. (Color online) Relaxation rate vs anisotropy in QDs. We choose $B = 3T$, $\ell_0 = 10$ nm, $\lambda_R = \lambda_D = 1.7$ μm, and $a = 5$. Here we define $\lambda_R = \hbar^2/m\alpha_R$, $\lambda_D = \hbar^2/m\alpha_D$, $E_x = \hbar\omega_0\sqrt{a}$, and $E_y = \hbar\omega_0\sqrt{b}$. The choice of these parameters mimics the experimentally reported values in Ref. 15. It can be seen that the theoretically obtained spin-relaxation rate is in excellent agreement with the experimentally reported values in Ref. 15. For symmetric QDs, (lower panel, inset plot), we chose $a = b = 5$.

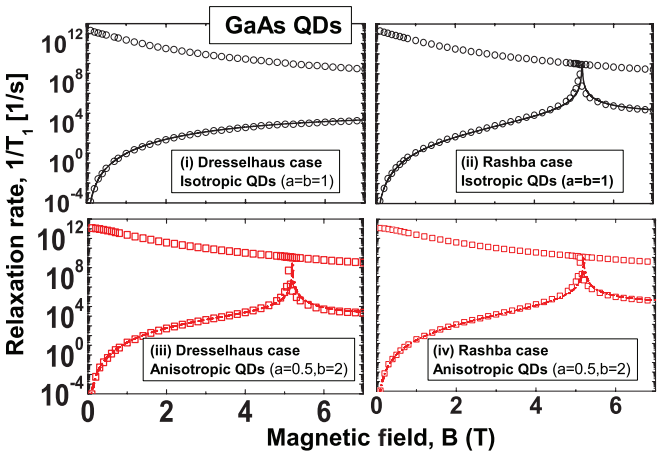

FIG. 3. (Color online) Contributions of the Rashba and the Dresselhaus spin-orbit coupling to the phonon induced spin-flip rate as a function of magnetic fields. Material constants are chosen the same as in Fig. 1, but $\hbar\omega_0 = 1.1$ meV and $\lambda_R = \lambda_D = 8$ μm. Solid lines (blue) are obtained from Eq. (17). Open circles and squares are obtained numerically from Eq. (16) by an exact diagonalization scheme implemented via finite element method.[41] Notice that a cusplike structure can be seen for the pure Dresselhaus case in asymmetric QDs [Fig. 2(iii), $a \neq b$] but not for symmetric QDs [Fig. 2(i), $a = b$]. Also, the spin-flip rate vanishes like B^5 [see Eq. (25)]. Figure 2(i) is the Loss *et al.* proposal for symmetric QDs (see Ref. 34). Figure 2(iii) is our proposal for asymmetric QDs. We also expect a similar cusplike structure for the pure Dresselhaus case with heavy holes in asymmetric QDs, which is different from Ref. 34.

accidental degeneracy even for the pure Dresselhaus spin-orbit coupling case in the phonon mediated spin-flip rate. This will be separately discussed from Figs. 3–7.

In Fig. 3(i) we see that the cusplike structure is absent (i.e., the spin-flip rate is a monotonous function of the magnetic field) for the pure Dresselhaus case in symmetric QDs. However in Fig. 3(iii) we see that the cusplike structure is present for the pure Dresselhaus case in asymmetric QDs. In Fig. 4, again we see that the cusplike structure is absent in isotropic QDs ($a = b$) but is present in anisotropic QDs

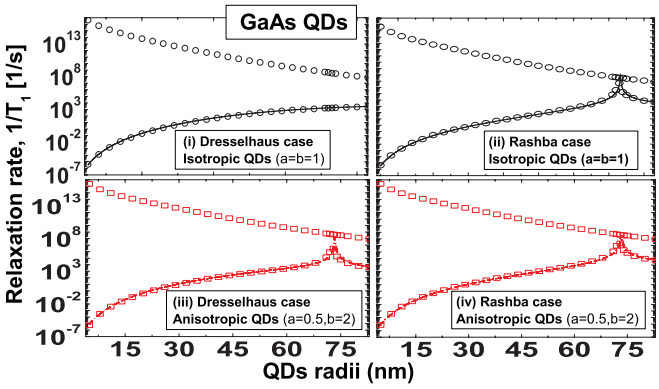

FIG. 4. (Color online) Same as Fig. 2 but $1/T_1$ vs ℓ_0. Here we chose $B = 1T$. Again, notice that the cusplike structure can only be seen for the pure Dresselhaus case in asymmetric QDs [Fig. 3(iii), $a \neq b$] but not for symmetric QDs [Fig. 3(i), $a = b$]. Also, the spin-flip rate vanishes like ℓ_0^8 [see Eq. (25)].

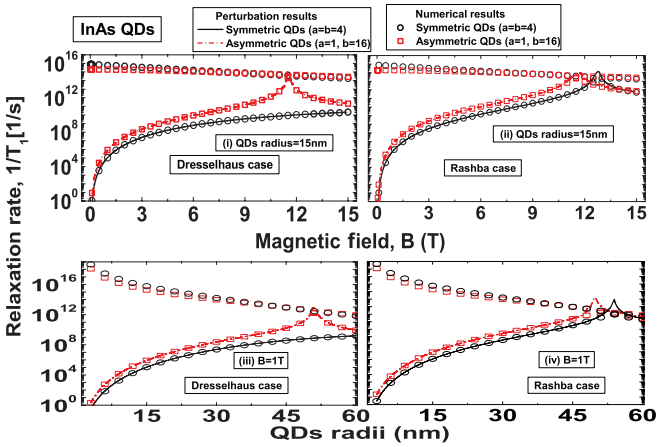

FIG. 5. (Color online) Same as Figs. 2 and 3 but for InAs QDs. We chose $E = 10^5$ V/cm. Again, notice that the cusplike structure can also be seen for the pure Dresselhaus case in asymmetric QDs ($a \neq b$) but not for symmetric QDs ($a = b$).

($a \neq b$) for the pure Dresselhaus case. The cusplike structure in anisotropic QDs is thus due to the fact that the anisotropy induces the accidental degeneracy in the matrix elements $[M(\mathbf{q}\alpha)]$ near the level crossing or anticrossing point. The accidental degeneracy point where the cusplike structure appears is referred to as the spin hot spot, while tuning on the spin-orbit coupling removes the degeneracy.[46] Thus, we apply degenerate perturbation theory, and the energy spectra of the unperturbed spin states $|0,0,-\rangle$ and $|0,1,+\rangle$ for anisotropic QDs are given by

$$\varepsilon^0_{0,0,-} = \tfrac{3}{2}\hbar\omega_+ - \tfrac{1}{2}\hbar\omega_- + \left(\alpha_R^2\xi_- + \alpha_D^2\zeta_-\right)^{1/2}, \quad (29)$$

$$\varepsilon^0_{0,1,+} = \tfrac{3}{2}\hbar\omega_+ - \tfrac{1}{2}\hbar\omega_- - \left(\alpha_R^2\xi_- + \alpha_D^2\zeta_-\right)^{1/2}. \quad (30)$$

We have substituted Eqs. (29) and (30) into Eq. (17) and found the spin-flip rate at the level crossing point from

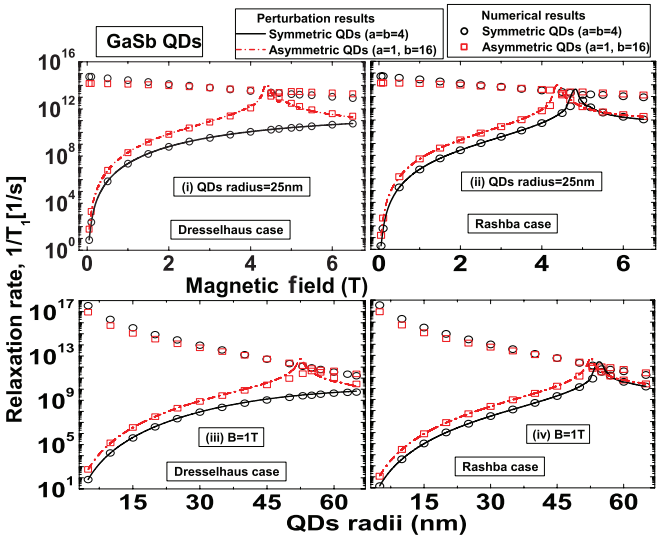

FIG. 6. (Color online) Same as Figs. 2 and 3 but for GaSb QDs. We chose $E = 10^5$ V/cm. Again, notice that the cusplike structure can also be seen for the pure Dresselhaus case in asymmetric QDs ($a \neq b$) but not for symmetric QDs ($a = b$).

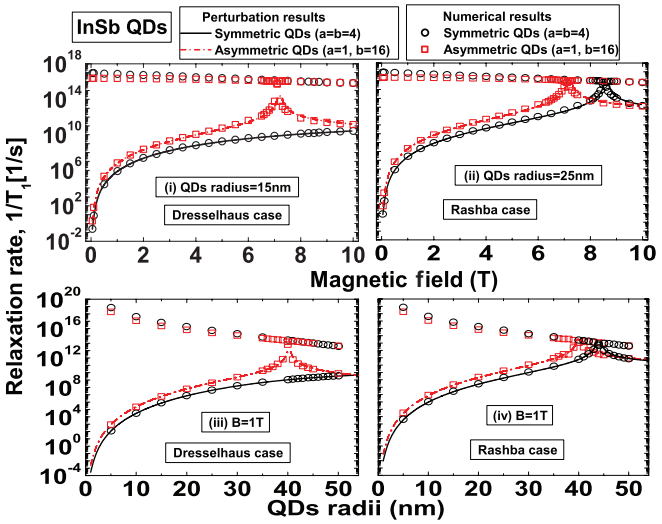

FIG. 7. (Color online) Same as Figs. 2 and 3 but for InSb QDs. We chose $E = 10^4$ V/cm. Again, notice that the cusplike structure can also be seen for the pure Dresselhaus case in asymmetric QDs ($a \neq b$) but not for symmetric QDs ($a = b$).

Figs. 2–7. Lifting the degeneracy with the application of spin-orbit coupling mixes spin-up and spin-down states where the phonon mediated spin transition rate between states of opposite magnetic moment will involve spin flips with a much more enhanced probability compared to the normal states. For example, the spin hot spot for the pure Dresselhaus case in symmetric GaAs QDs [Figs. 3(i) and 4(i)] cannot be observed while tuning the anisotropy ($a \neq b$) but can be observed at $B = 5.1T$ and $\ell_0 = 69$ nm, as shown in Figs. 3(iii) and 4(iii), respectively. Notice that the spin-flip rates of the pure Dresselhaus case found near the spin hot spot in Figs. 3(iii) and 4(iii) are six orders of magnitude larger than those values found in Figs. 3(i) and 4(i). This result (i.e., the spin hot spot in asymmetric QDs for the pure Dresselhaus case yet to be experimentally verified) provides small relaxation and decoherence times, which should be avoided during the design of spin based transistors for possible implementation in quantum logic gates, quantum computing, and quantum information processing. From Figs. 4–7, we investigated the spin-relaxation rate in InAs, GaSb, and InSb QDs. Analyzing all plots, the spin hot spot and associated cusplike structure can be seen in the pure Dresselhaus spin-orbit coupling case in anisotropic QDs ($a \neq b$).

TABLE I. The material constants used in our calculations, taken from Refs. 26 and 47.

Parameters	GaAs	InAs	GaSb	InSb
g_0	−0.44	−15	−7.8	−50.6
m	0.067	0.0239	0.0412	0.0136
γ_R (Å^2)	4.4	110	33	500
γ_D (eV Å^3)	26	130	187	228
eh_{14} (10^{-5} erg/cm)	2.34	0.54	1.5	0.75
s_l (10^5 cm/s)	5.14	4.2	4.3	3.69
s_t (10^5 cm/s)	3.03	2.35	2.49	2.29
ρ (g/cm^3)	5.3176	5.667	5.6137	5.7747

V. CONCLUSIONS

We have shown that the anisotropy breaks the in-plane rotational symmetry. As a result, we found that the cusplike structure (i.e., where the spin hot spot is located) is present in the phonon mediated spin transition rate in anisotropic QDs for the pure Dresselhaus spin-orbit coupling case. In contrast, for isotropic QDs, the spin transition rate is a monotonous function of magnetic fields and QD radii (i.e., where the spin hot spot is absent) for the pure Dresselhaus spin-orbit coupling case. These results (yet to be experimentally verified) provide information for finding the spin hot spot in anisotropic spin relaxation for the pure Dresselhaus case during the design of QD spin transistors. At or nearby the spin hot spot, the relaxation and decoherence time are smaller by several orders of magnitude. One should avoid such locations during the design of QD spin based transistors for possible implementation in quantum logic gates, quantum computing, and quantum information processing.

ACKNOWLEDGMENTS

This work has been supported by Natural Science and Engineering Research Council (Canada) and Canada Research Chair programs. The authors acknowledge the Shared Hierarchical Academic Research Computing Network community and Dr. Philip James Douglas Roberts for the helpful and technical support.

[1] D. Loss and D. P. DiVincenzo, Phys. Rev. A **57**, 120 (1998).
[2] D. D. Awschalom, D. Loss, and N. Samarth, *Semiconductor Spintronics and Quantum Computation* (Springer, Berlin, 2002).
[3] R. Hanson, L. H. W. van Beveren, I. T. Vink, J. M. Elzerman, W. J. M. Naber, F. H. L. Koppens, L. P. Kouwenhoven, and L. M. K. Vandersypen, Phys. Rev. Lett. **94**, 196802 (2005).
[4] M. Kroutvar, Y. Ducommun, D. Heiss, M. Bichler, D. Schuh, G. Abstreiter, and J. J. Finley, Nature (London) **432**, 81 (2004).
[5] J. M. Elzerman, R. Hanson, L. H. Willems van Beveren, B. Witkamp, L. M. K. Vandersypen, and L. P. Kouwenhoven, Nature (London) **430**, 431 (2004).
[6] M. Glazov, E. Sherman, and V. Dugaev, Physica E **42**, 2157 (2010).
[7] J. I. Climente, A. Bertoni, G. Goldoni, M. Rontani, and E. Molinari, Phys. Rev. B **75**, 081303 (2007).
[8] P. Pietiläinen and T. Chakraborty, Phys. Rev. B **73**, 155315 (2006).
[9] T. Chakraborty and P. Pietiläinen, Phys. Rev. Lett. **95**, 136603 (2005).
[10] M. P. Nowak and B. Szafran, Phys. Rev. B **83**, 035315 (2011).
[11] M. P. Nowak and B. Szafran, Phys. Rev. B **80**, 195319 (2009).
[12] M. P. Nowak and B. Szafran, Phys. Rev. B **81**, 235311 (2010).
[13] V. N. Golovach, A. Khaetskii, and D. Loss, Phys. Rev. Lett. **93**, 016601 (2004).
[14] X. Wang, L. S. Bishop, J. Kestner, E. Barnes, K. Sun, and S. Das Sarma, Nat. Commun. **3**, 997 (2011).
[15] S. Amasha, K. MacLean, I. P. Radu, D. M. Zumbühl, M. A. Kastner, M. P. Hanson, and A. C. Gossard, Phys. Rev. Lett. **100**, 046803 (2008).
[16] S. Bandyopadhyay, Phys. Rev. B **61**, 13813 (2000).
[17] T. Fujisawa, Y. Tokura, and Y. Hirayama, Phys. Rev. B **63**, 081304 (2001).
[18] A. Balocchi, Q. H. Duong, P. Renucci, B. L. Liu, C. Fontaine, T. Amand, D. Lagarde, and X. Marie, Phys. Rev. Lett. **107**, 136604 (2011).
[19] M. Griesbeck, M. M. Glazov, E. Y. Sherman, D. Schuh, W. Wegscheider, C. Schüller, and T. Korn, Phys. Rev. B **85**, 085313 (2012).
[20] O. Olendski and T. V. Shahbazyan, Phys. Rev. B **75**, 041306 (2007).
[21] M. E. Flatté, Physics **4**, 73 (2011).
[22] Y. A. Bychkov and E. I. Rashba, J. Phys. C **17**, 6039 (1984).
[23] G. Dresselhaus, Phys. Rev. **100**, 580 (1955).
[24] S. Prabhakar and J. E. Raynolds, Phys. Rev. B **79**, 195307 (2009).
[25] S. Prabhakar, J. Raynolds, A. Inomata, and R. Melnik, Phys. Rev. B **82**, 195306 (2010).
[26] R. de Sousa and S. Das Sarma, Phys. Rev. B **68**, 155330 (2003).
[27] S. Prabhakar, R. V. N. Melnik, and L. L. Bonilla, Appl. Phys. Lett. **100**, 023108 (2012).
[28] J. A. Folk, S. R. Patel, K. M. Birnbaum, C. M. Marcus, C. I. Duruöz, and J. S. Harris, Phys. Rev. Lett. **86**, 2102 (2001).
[29] T. Fujisawa, D. G. Austing, Y. Tokura, Y. Hirayama, and S. Tarucha, Nature (London) **419**, 278 (2002).
[30] R. Hanson, B. Witkamp, L. M. K. Vandersypen, L. H. W. van Beveren, J. M. Elzerman, and L. P. Kouwenhoven, Phys. Rev. Lett. **91**, 196802 (2003).
[31] C. E. Pryor and M. E. Flatté, Phys. Rev. Lett. **96**, 026804 (2006).
[32] C. E. Pryor and M. E. Flatté, Phys. Rev. Lett. **99**, 179901(E) (2007).
[33] M. P. Nowak, B. Szafran, F. M. Peeters, B. Partoens, and W. J. Pasek, Phys. Rev. B **83**, 245324 (2011).
[34] D. V. Bulaev and D. Loss, Phys. Rev. Lett. **95**, 076805 (2005).
[35] D. V. Bulaev and D. Loss, Phys. Rev. B **71**, 205324 (2005).
[36] C. Yang, A. Rossi, R. Ruskov, N. Lai, F. Mohiyaddin, S. Lee, C. Tahan, G. Klimeck, A. Morello, and A. Dzurak, arXiv:1302.0983.
[37] W. Peng, Z. Aksamija, S. A. Scott, J. J. Endres, D. E. Savage, I. Knezevic, M. A. Eriksson, and M. G. Lagally, Nat. Commun. **4**, 1339 (2013).
[38] T. S. Koh, J. K. Gamble, M. Friesen, M. A. Eriksson, and S. N. Coppersmith, Phys. Rev. Lett. **109**, 250503 (2012).
[39] Z. Shi, C. B. Simmons, J. R. Prance, J. K. Gamble, T. S. Koh, Y.-P. Shim, X. Hu, D. E. Savage, M. G. Lagally, M. A. Eriksson, M. Friesen, and S. N. Coppersmith, Phys. Rev. Lett. **108**, 140503 (2012).
[40] J. R. Prance, Z. Shi, C. B. Simmons, D. E. Savage, M. G. Lagally, L. R. Schreiber, L. M. K. Vandersypen, M. Friesen, R. Joynt, S. N. Coppersmith, and M. A. Eriksson, Phys. Rev. Lett. **108**, 046808 (2012).
[41] Comsol Multiphysics version 3.5a (www.comsol.com).
[42] A. V. Khaetskii and Y. V. Nazarov, Phys. Rev. B **61**, 12639 (2000).
[43] S. Prabhakar, J. E. Raynolds, and R. Melnik, Phys. Rev. B **84**, 155208 (2011).
[44] A. V. Khaetskii and Y. V. Nazarov, Phys. Rev. B **64**, 125316 (2001).
[45] V. F. Gantmakher and Y. B. Levinson, *Carrier Scattering in Metals and Semiconductor* (North-Holland, Amsterdam, 1987).
[46] P. Stano and J. Fabian, Phys. Rev. B **74**, 045320 (2006).
[47] M. Cardona, N. E. Christensen, and G. Fasol, Phys. Rev. B **38**, 1806 (1988).